

# OPEN-FORMAT PRESCRIPTION MAPS FOR VARIABLE RATE SPRAYING IN ORCHARD FARMING



Francisco Rovira-Más<sup>1,\*</sup>, Verónica Saiz-Rubio<sup>1</sup>, Andrés Cuenca<sup>1</sup>, Coral Ortiz<sup>1</sup>, Montano Pérez Teruel<sup>1</sup>, Enrique Ortí<sup>1</sup>

<sup>1</sup> Agricultural Robotics Laboratory, Universitat Politècnica de Valencia, Spain.

\* Correspondence: frovira@dmta.upv.es

## HIGHLIGHTS

- Straightforward procedure to code prescription maps independent of manufacturers.
- Methodology suitable for orchard crops and vineyards including pressures up to 10 bar and flowrates up to 100 L/min.
- Algorithm validated for both trellis-based continuous rows and traditional orchard rows of discrete trees.
- Method scalable to other agricultural operations, such as fertilizing or data registration for auditing purposes.


**ABSTRACT.** *The implementation of crop protection solutions contributing to significant reductions in the use and risk of chemical pesticides has motivated the interest of site-specific systems, such as variable rate technologies based on user-set prescriptions. However, the practical implementation of variable rates has been dissuasive for many growers who are not familiar with digital solutions, as proprietary firmware is often difficult to grasp. This paper presents a method for formatting prescription maps that is independent of manufacturers, can be easily and freely implemented by industry and can be adopted by growers not familiar with advanced software tools. The methodology was successfully demonstrated for perennial specialty crops, in particular for trellised vineyards in vertical shoot position and for traditional olive groves. Results showed that the variations within user prescription maps were translated to the fields, but flow errors appeared due to the challenge of measuring flow and pressure in the highly pulsating actuation of pulse-width-modulated (PWM) valves. Such errors diminished with the use of low-volume rates and the optimal selection of the nozzles when adjusted to the real pressure measured in the field. The use cases validated in the field showed the consistency of the method for highly populated prescription maps of 1,221 points/ha accessible to advanced farmers, as well as for modest maps of 80 points/ha within reach of the majority of growers.*

**Keywords.** *Automated map building, Local tangent plane coordinates, Orchard crop operations, Precision farming, Prescription maps, User-centered approach, Variable rate spraying.*

The Legally Binding Targets that will be laid down in a regulation on all European Union Member States, in draft status at present, have instructed the implementation of crop protection solutions contributing to a 50% reduction in the use and risk of chemical pesticides by 2030. This policy, and similar ones in other countries, have resulted in the development of technologies leading to a more rational application of spraying products in the context of precision agriculture and, in particular, a growing interest in variable rate technologies (VRT). Such technologies allow for a more accurate delivery of spray droplets and systematic ways of data collection for auditing

and reporting purposes. The problem of effective, while sustainable, crop protection is particularly critical for the case of orchard crops, where pests are strongly attracted by fruits, and pest attacks typically leave crops without commercial value as market standards for fresh produce are usually high. Specialty crops are intensive, high-value crops that include fruits, vegetables, tree nuts, and dried fruits, as well as horticulture and floriculture. In Europe, specialty crops are valued at about €70 billion per year, representing 22% of the total output value of the agricultural sector. In particular, the production of oranges in 2022 reached 6.2 million ton equivalent to €1.9 billion, nectarines and peaches accounted for 4.1 million ton and €3.7 billion, olives totaled 10.9 million ton and €2.3 billion, and grapes for wine led to 178 million hl and €8.7 billion (FAO, 2023). In the USA, specialty crop production represents approximately 50% of the total value of crop production, with a retail value for 2005 of around \$60 billion (Burks et al., 2008).

The benefits of VRT have been reported to approximate the reduction challenges posed by the crop protection policies of the European Union, the USA, and many other countries with similar environmental laws. Yang et al. (2018), for

 The authors have paid for open access for this article. This work is licensed under a Creative Commons Attribution-NonCommercial-NoDerivatives 4.0 International License <https://creativecommons.org/licenses/by-nc-nd/4.0/>

Submitted for review on 27 July 2023 as manuscript number ITSC 15750; approved for publication as a Research Article by Associate Editor Prof. Brian Steward and Community Editor Dr. Seung-Chul Yoon of the Information Technology, Sensors, & Control Systems Community of ASABE on 22 December 2023.

instance, effectively controlled cotton root rot with fungicide reductions over 40%. Such savings can be applied in practice by two approaches within VRT: 1) by applying a prescription map built and uploaded before the treatment; and 2) by sensing and processing crop features in real time. Given that weed patches are relatively immobile in fields, Brown and Stecklen (1995) applied prescribed maps to reduce herbicide amounts with spatially variable spraying. However, despite successful implementations over the last two decades, the adoption rate of VRT is still low. Masi et al. (2023) recently reported that North American farms are more likely to use VRT than European farms, and yet VRT utilization rates in the USA hardly exceed 40%, whereas in Europe, its uptake rarely exceeds 20%. In fact, although cotton growers are aware that only patches are infested, they apply fungicide uniformly because (among other reasons) prescription maps and VRT equipment are not readily available (Yang et al., 2018). As a result, there is a need for developing standardized procedures capable of creating prescription maps and adapting VRT to existing machinery. In a survey conducted in Italy (Masi et al., 2023), where fruit and vegetables were the dominant crops (58%), farmer age, equipment cost, and farm size were found to strongly influence the VRT adoption rate, in addition to system complexity. Yang et al. (2018) also concluded that variable rate applications require more advanced computer and equipment skills, as well as a better understanding of the techniques involved, which often results in the need of assistance from dealers or service providers to actually draw prescription maps and effectively apply VRT. The fact that the adoption of VRT in Europe rarely exceeds 20% and is half the rate found in the USA may be induced by the weight of family-based small-scale farmers in European agriculture. A standard procedure to code maps that is independent of manufacturers, and therefore can be implemented with the machinery already existing in the farm can reduce the impact of technology cost as a barrier for VRT uptake, even though the average age of professional farmers in Europe is still an obstacle for widespread farm digitization.

The advantages of mapping the fields ahead of time to code application rates into a prescription map are often canceled out by the difficulty of creating and transferring a prescription map to a machine enabled to deliver variable rates, as map configuration depends on equipment manufacturers. As explained by Norwood et al. (2009) and confirmed by Song et al. (2012), one must know what computer and controller will be used to create a prescription map in the appropriate format, such as “.tgt” for Ag Leader (PF3000 Pro) or “.shp” for Raven (Viper), for example. Furthermore, some controllers, such as those made by John Deere, require a boundary file of the field in addition to the prescriptions. Due to the lack of standardization, and thus a consensus among manufacturers and practitioners, some commercial solutions have borrowed GIS formats such as “.geojson” and “.json.” It is here, in the core of prescription coding, where the requirement of advanced computer and equipment skills mentioned by Yang et al. (2018) fits into place, providing thus a motivation for finding new ways of coding prescription maps that are independent of specific manufacturers. The calculation of prescriptions is based on data collected

from the field, and the nature of these data depends on the type of application. For example, Brown and Stecklen (1995) used conventional color and infrared images taken from a low altitude (900 m) aircraft to apply herbicide to weed patches with a ground sample distance (GSD) of  $10 \times 10 \text{ cm}^2/\text{pix}$ ; Norwood et al. (2009) outlined prescription maps of fertilizer according to soil test results; Song et al. (2012) combined soil sampling, NDVI, and historical records to produce prescription maps for variable rate aerial spraying; Yang et al. (2018) effectively controlled cotton root rot with site-specific fungicide application at planting based on airborne imagery acquired from a Cessna 206 aircraft with a four-camera imaging system providing images ( $2048 \times 2048$  pixels) in the blue, green, red, and infrared bands; and Li et al. (2019) calculated fertilizing rates based on the nutritional status of corn estimated from photos taken in the field with a handheld digital camera. Even though the process of determining rates from field data is important for VRT, it is not central to *map construction and interpretation by machines*, which is where the lack of standardization rests. As a result, this paper will focus on map coding and configuration rather than the calculation of rates, which depends on each particular application (spraying, seeding, fertilizing, irrigation, etc.) and thus falls outside of the scope of this article.

The steps typically followed to create prescription maps include map zoning, although there is no one single approach specifically to doing it (Song et al., 2012). For prescriptions to be based on zones, the first step is to delineate the zones with specialized software packages (Yang et al., 2018), which may be dissuasive for many growers. Each zone represents a rate, for example, Yang et al. (2018) reduced the map to a binary prescription of fungicide of 0 L/ha and 56 L/ha, whereas Li et al. (2019) implemented three fertilizing levels of 200 kg/ha, 250 kg/ha, and 300 kg/ha. The division of the field into a predetermined number of zones requires a previous discretization of the terrain because global positioning receivers provide locations for single points. Such discretization is normally embodied in grids, which are the basis of the methodology proposed in this research. Polygons smaller than  $4 \text{ m}^2$  within dominant zones were considered belonging to the dominant class by Yang et al. (2018), whereas Norwood et al. (2009) typically divided fields into 2.5-acre ( $10,117 \text{ m}^2$ ) grids, and Brown and Stecklen (1995) implemented a grid size of 6 m x 15 m ( $90 \text{ m}^2$  cells) using GIS software (PC ARC/INFO v 3.3) for weed mapping. The layout of prescription maps is governed by resolution, and therefore this is a key parameter to set at the time of building a map. The fact that efficient maps have been reported with cell sizes ranging from  $4 \text{ m}^2$  to  $10,117 \text{ m}^2$  ( $\approx 1 \text{ ha}$ ) implies that resolution will be dependent on each particular application.

At the time of coding a prescription map, the user must consider that the prescribed rates have to be physically applied by an automated machine, and therefore physical variables such as vehicle velocity, flow inertia, and flow-pressure relationships for liquids need to be taken into account. Norwood et al. (2009) clearly stated that each executing controller must be known to create a particular prescription map. In the case of prescription-based variable rate spraying

developed in this research, understanding how spray flow varied on-the-fly resulted was for the successful implementation of the proposed prescription maps. In consequence, although out of the scope of this paper, some basic background on smart spraying actuation is necessary. The key idea for smart spraying is to vary the spray flow according to the prescription preset for a given location of the sprayer without altering the droplet size. Wrong droplet size results in spray drift or runoff (Rathnayake et al., 2022), which opposes the current policies of environmental protection agencies. Keeping the droplet size within a limited range requires keeping the system pressure within a limited range (Fabula et al., 2021), which is the central problem of variable rate sprayers. Boom sprayers for herbicide application have solved the problem with the introduction of pulse width modulated (PWM) solenoid valves, which can vary the sprayed flow by changing the duty cycle of a square signal (Han et al., 2001). Such technical success has motivated the replication of this philosophy for orchard sprayers (Salcedo et al., 2020; Rathnayake et al., 2022; Ortí et al., 2022). However, such adaptation is not straightforward, because when PWM valves are implemented in air blast sprayers featuring a larger working pressure and high flow variations, the spray flow becomes turbulent by the highly pulsating system and forces hydraulic shocks when full valve closures are ordered (Saiz-Rubio et al., 2023; Ortiz et al., 2023). This phenomenon is especially acute in relation to pressure sensors and flowmeters, as smart sprayers must grant both, a system pressure within setup limits and a sprayed flow near the prescribed rate, and none of them can be granted unless onboard sensors work properly. This problem falls outside of the scope of this article but has to be kept in mind when evaluating the proposed methodology through the use cases of vineyards and olive groves.

The objectives of this paper are two: first, the introduction of a new method for formatting prescription maps; and second, its validation through two use cases applied to relevant crops. The key advantages of the proposed method are that it is independent of manufacturers, and therefore it can be easily implemented by industry and freely adopted by growers.

## METHODOLOGY

### USER-ORIENTED FORMAT

The distinctive features of the proposed format for coding variable rate prescriptions are the simplicity for the user and the independence of maps from manufacturers, such that machine operators easily instructed on interpreting a digital map from a field can compose a prescription map, and any

manufacturer implementing VR technology can write a straightforward software application to read it. The next paragraph explains how a grower can write a prescription map following the proposed format, and the next section describes in detail how any machine can easily read the maps and execute a variable rate treatment.

The approach to defining this format follows a bottom-up direction by which grower knowledge and needs are directly transcribed into a text file. In particular, grower knowledge is bound to the crop and the plot, and it refers to the rate that every section of the field needs, where the size and number of sections, as well as the preferred rate for them, is a decision made by the grower. In practical terms, it requires two pieces of information: field locations given by three GNSS coordinates (latitude, longitude, and altitude) and the spray rates associated to them in common units, for example,  $L \cdot \text{min}^{-1}$ . As a result, these are the specific data that growers need to write in the map, following the orderly manner of figure 1. The number of points (NP) will depend on the number and distribution of rates chosen for a given treatment. As variability increases, it is recommendable to increase the number of points accordingly, but the precision embodied in each map will eventually be a decision made by each grower. As a rule of thumb, it is recommended to have at least 100 points/ha and no less than 50 points/ha. Likewise, latitude and longitude should have at least seven decimals to grant enough accuracy (the system implemented in the use cases described below works with 10 decimals). In addition, notice that west longitudes and south latitudes must be negative.

The text file of figure 1b can be easily written in any word processor, and the key question for the grower is how to determine the numbers that fill the columns of the table of figure 1a. As growers typically know their fields well, they will be able to tag points representing important sections of the field and extract the GNSS (often GPS) coordinates of latitude, longitude, and altitude. This can be performed with any digital mapping tool, from GIS software run on a computer to Google Maps accessed from a common smartphone. A more delicate decision, however, is how to set the rates for each section to comply with spraying regulations. Multiple strategies can be followed with this regard, although the maximum rates must be acceptable by regulatory bodies. However, efficiency may be greatly improved by lowering rates for specific zones based on prior phytosanitary knowledge acquired in the field or based on the canopy thickness when tree development has not been homogeneous within the field. The simple layout of figure 1 can produce highly precise maps with different levels of resolution. Users can adjust the number of points from a basic representation of 100 points/ha up to plant-specific accuracy, which allows

NP (positive integer)									
Lat <sub>1</sub>	<i>Tab</i>	Lon <sub>1</sub>	<i>Tab</i>	Alt <sub>1</sub>	<i>Tab</i>	Rate <sub>1</sub>			
Lat <sub>2</sub>	<i>Tab</i>	Lon <sub>2</sub>	<i>Tab</i>	Alt <sub>2</sub>	<i>Tab</i>	Rate <sub>2</sub>			
Lat <sub>3</sub>	<i>Tab</i>	Lon <sub>3</sub>	<i>Tab</i>	Alt <sub>3</sub>	<i>Tab</i>	Rate <sub>3</sub>			
.		.		.		.			
.		.		.		.			
.		.		.		.			
Lat <sub>NP</sub>	<i>Tab</i>	Lon <sub>NP</sub>	<i>Tab</i>	Alt <sub>NP</sub>	<i>Tab</i>	Rate <sub>NP</sub>			

(a)

36									
39.4829175		-0.337570611		5.007		10			
39.4829515		-0.337544528		5.644		15			
39.48298286		-0.337520667		5.523		20			
39.48302314		-0.337485611		5.477		25			
39.48305181		-0.337461		5.401		30			
39.48308036		-0.3374305		5.332		35			
39.48312553		-0.337397944		5.226		40			
39.48315628		-0.337362556		5.491		45			

(b)

Figure 1. Writing format for proposed prescription maps: (a) formatting style; (b) example.

them to control the precision of their treatments. As prescription maps are written and recorded in a plain text processor, they can be easily read from a computer folder set in the sprayer computer. Likewise, the reduced size of text-coded data also facilitates file sending and handling among diverse machine operators.

### EXECUTION OF SITE-SPECIFIC PRESCRIPTIONS

A prescription map for commanding variable rate spraying requires two pieces of information: 3D field positions and the desired rate for them (the four columns in fig. 1b). The way of coding this information in the prescription maps is crucial for their further adoption by typical operators with basic computer skills. Additionally, a straightforward translation of field needs using grower language contributes to the ultimate objective of efficiently adjusting spray amount to actual crop needs. The following paragraphs of this section explain the key features of the proposed methodology, by which users only have to provide a number of points (NP) with a reference location and a desired spray rate (fig. 1).

Field positioning requires the use of a global navigation satellite system (GNSS) receiver, which is easily available in a wide range of costs and performance capabilities to fulfill any need found in the field. Nevertheless, the signal-blocking canopies of many orchard crops and the responsibility of avoiding overspraying advise farmers to invest in reliable receivers within users' affordability. Whereas there is a consensus about the source of positioning data from GNSS receivers, the way to handle such data does not follow a standard procedure, and in fact, this has been dissuasive for the widespread adoption of precision agriculture in orchard crops. Although receivers estimate other parameters in addition to position and time, such as heading or velocity, prescription maps only require global positioning, and therefore only the coordinates of field points will be considered in relation to GNSS data for the scope of this work. All GNSS receivers provide real-time positioning in geodetic coordinates latitude ( $\lambda$ ), longitude ( $\phi$ ), and altitude ( $h$ ). However, spherical coordinates  $\lambda$  and  $\phi$  measured in degrees and referenced to the Earth's center of mass (fig. 2a) are counterintuitive for the terrains of limited dimensions typically covered by agricultural equipment such as sprayers. Furthermore, the conventional calculation of areas and distances in farm plots relies on Euclidean geometry, which cannot be

used with spherical coordinates latitude and longitude. Thus, a coordinate transformation from geodetic to flat Cartesian coordinates is necessarily the first stage of this mapping method, as embodied in the algorithm of figure 3. Universal Transverse Mercator (UTM) coordinates are popular flat coordinates among GIS practitioners, but they are represented by large numbers with an origin of coordinates unknown to the users, which are still not intuitive enough for field-based operators. To overcome this disadvantage, the methodology proposed in this paper departs from this regular practice by introducing local tangent plane (LTP) coordinates, also called *locally level coordinates*, which use common metric length units (m), east-north orientation for x-y Cartesian coordinates, and a local origin chosen by each user according to preferences and convenience (fig. 2c). The mathematical transformation from geodetic (e.g., GNSS native) to LTP coordinates requires an intermediate step through the earth-centered-earth-fixed (ECEF) coordinates ( $X, Y, Z$ ) of figure 2b, and can be consulted in Grewal et al. (2001) or easily followed step by step in Rovira-Más et al. (2010). Notice that such a transformation requires the selection of an Earth model to determine the axes and eccentricity of the geoid. Within the scope of this research, the World Geodetic System 1984 (WGS 84) has been used as Earth model. Figure 2

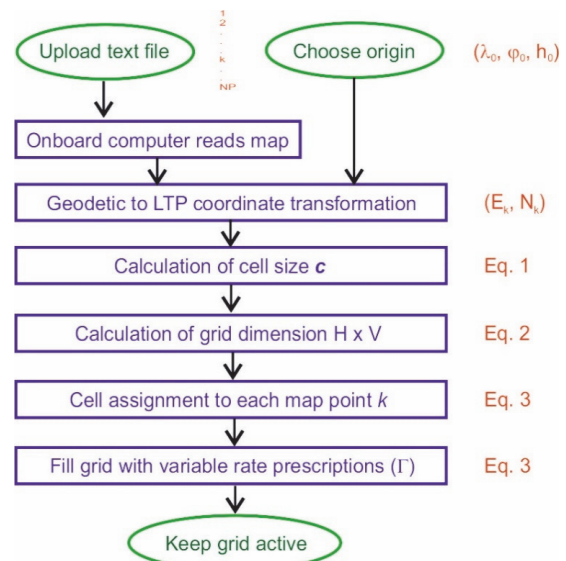


Figure 3. Construction algorithm for open-format prescription maps.

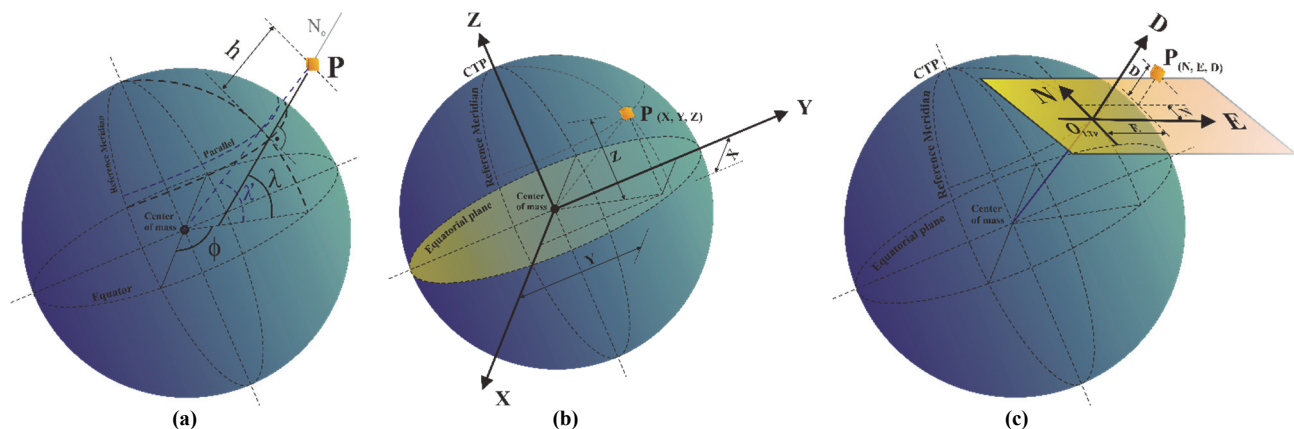


Figure 2. GNSS coordinate systems: (a) geodetic; (b) ECEF; (c) LTP.



represents the initial geodetic system in which GNSS coordinates are expressed (a), the intermediate ECEF coordinate system with Cartesian coordinates and origin at the center of mass of the Earth (b), and the final LTP coordinate system with flat Cartesian coordinates north-east and user-selected origin O (c) for a given point P.

The transformation to LTP coordinates ( $E_k, N_k, h_k$ ) assures a practical coordinate origin and therefore convenient coordinates in the east and north directions (fig. 2c) for any plot location (figs. 7a and 13a). As the choosing of an origin by the grower is only conducted once and kept unchanged, data can be compared among different years.

It is impossible to set up a prescription map that contains all the waypoints through which the sprayer might go in the future, regardless of equipment and operator. As a result, the map must not only be time-invariant but also accommodate for trajectory deviations and diverse resolutions in the definition of the spray rates. Both conditions can be met when the physical reality of the field is systematically discretized into a regular grid, whose cells represent the spray rate prescribed for each location. For this layout, though, the dimension of the cell is an important parameter to decide because it establishes the resolution of the map. With this regard, two options were considered: a) the user decides the size of the cell based, for instance, on the row spacing; and b) the algorithm calculates the optimal cell size that provides full coverage of the field, such that every cell containing vegetation has at least one rate prescription (this was the default option as indicated in fig. 3). If locations tagged with a prescription are far apart because row spacing is large compared to tree spacing, or the user has manually selected a small cell size, there will be empty cells in the middle of the prescribed cells. Equation 1 indicates how the algorithm automatically calculates the cell size ( $c$ ) as a function of the dimensions of the field (maximum and minimum LTP coordinates) and the number of points (NP). Note that  $c$  must be a positive integer, and the smallest cell considered by the algorithm is  $1 \times 1 \text{ m}^2$  for practical purposes.

$$c = \left\lceil \sqrt{\frac{(E_{\max} - E_{\min}) \cdot (N_{\max} - N_{\min})}{\text{NP}}} \right\rceil \quad \begin{array}{l} \text{NP} > 0 \\ c \in \mathbf{N}; c \geq 1 \end{array} \quad (1)$$

Once the size of the field in the north and east directions has been estimated and the cell size defined, the following step in the algorithm is the actual construction of the prescription grid that will be executed by the smart sprayer. The dimensions of the square grid ( $H \times V$ ) that contains the field plot can be determined from equation 2, and the filling of the grid with the user-set prescriptions is immediate through equation 3,

where

( $E_k, N_k$ ) = LTP coordinates of point  $k$  from the prescription map composed by the grower (fig. 1b)

$R_k$  = spray rate set in the prescription map for point  $k$  (fig. 1b, last column)

( $H, V$ ) = horizontal ( $H$ ) and vertical ( $V$ ) dimension of the algorithm-generated grid in number of cells

( $i, j$ ) = horizontal ( $i$ ) and vertical ( $j$ ) indices of any cell belonging to the prescription grid

( $i_k, j_k$ ) = horizontal ( $i_k$ ) and vertical ( $j_k$ ) indices of the cell that contains point  $k$  of coordinates ( $E_k, N_k$ )

$\Gamma(i, j)$  = function that assigns a spray rate to cell location ( $i, j$ ).

Notice that the final rate assigned by function  $\Gamma$  considers the possibility of various rates being assigned by the grower to the same physical cell. For such a case, the final rate associated with the cell can be the average value of the rates whose point locations fall within the cell, the maximum rate among them, or any other combination that issues a rate physically reachable by the sprayer.

$$\begin{aligned} H &= \left\lceil \frac{E_{\max} - E_{\min}}{c} \right\rceil & H \in \mathbf{N} \\ V &= \left\lceil \frac{N_{\max} - N_{\min}}{c} \right\rceil & V \in \mathbf{N} \end{aligned} \quad (2)$$

$$i_k = \left\lceil \frac{E_k - E_{\min}}{c} \right\rceil \quad i_k \in \mathbf{N}; i_k \in [1, H]; k \in [1, \text{NP}]$$

$$j_k = \left\lceil \frac{N_k - N_{\min}}{c} \right\rceil \quad j_k \in \mathbf{N}; j_k \in [1, V]; k \in [1, \text{NP}]$$

$$\begin{cases} i = i_k \\ j = j_k \end{cases} \rightarrow \Gamma(i, j) = \begin{cases} \text{if } \Gamma(i, j) = 0 \rightarrow \Gamma(i, j) = R_k \\ \text{if } \Gamma(i, j) \neq 0 \rightarrow \Gamma(i, j) = \begin{cases} \max\langle \Gamma(i, j), R_k \rangle \\ \text{or} \\ \frac{R_k + \Gamma(i, j)}{2} \end{cases} \end{cases} \quad (3)$$

The algorithm sketched in figure 3 transforms the maps defined by users as a simple list written in a standard text file into a global-referenced grid containing spray rate prescriptions. The following paragraphs explain, along with figure 4, how any spray equipment can read and apply the user-set prescribed rates, providing a solid procedure for manufacturers to upgrade conventional equipment by enabling the real-time application of variable rates, and thus align themselves with the principles of precision farming and digital agriculture.

Before VRT-enabled machines can apply the rates coded in the maps, they need to know where they are located, and more importantly, they need to make sure that they are within the plot limits defined in the prescription map. Such a task is eased by the aforementioned transformation to LTP coordinates. Given that each user has already provided the position of a local origin for each plot, the GNSS coordinates sent continuously from the receiver installed in the vehicle ( $\lambda_k, \phi_k, h_k$ ) will be automatically transformed to LTP coordinates ( $E_k, N_k$ ) by the algorithm; as long as coordinates for point  $k$  are within the boundaries determined by ( $E_{\min}, E_{\max}$ ) in the east direction and ( $N_{\min}, N_{\max}$ ) in the north direction, the machine will be inside the plot, and therefore the map will be valid. Otherwise, a warning message stating that the sprayer is outside the plot will be issued, and the nozzles will

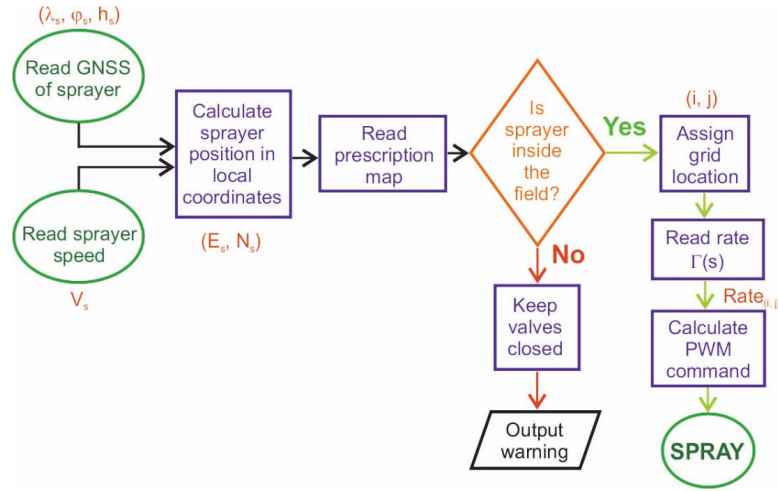


Figure 4. Equipment-embedded algorithm for the application of variable rate prescription maps.

be automatically deactivated. For every valid point  $(E_k, N_k)$ , there will be a corresponding grid location determined by  $(i_k, j_k)$  according to equation 3, which in turn will lead to a specific spray rate  $\Gamma(i, j)$ . The final step consists of transforming that particular rate expressed in flow units, such as  $L \cdot \text{min}^{-1}$ , into execution commands for the solenoid-driven nozzles of the sprayer. The function to drive such transformation will depend on each specific piece of equipment, in particular on the number and distribution of nozzles, the type of nozzle bodies (disc and core), the flow range, and the spraying strategy envisioned when sections of several nozzles are commanded independently. The way information has been coded in the maps allows for their generalized use in any kind of VRT machine beyond sprayers, such as fertilizers or seeding machines. The use cases developed below for vineyards and olive groves provide guiding examples of diverse transformation functions successfully adapted to the needs of each machine and crop.

#### IMPLEMENTATION OF VARIABLE RATE PRESCRIPTIONS WITH PWM TECHNOLOGY

The execution of a prescription map like the ones shown in figures 7 and 13 requires regulation of spray flow in real time, i.e., while the sprayer is in motion. Previous attempts before the advent of PWM-actuated nozzles used to regulate flow by changing the working pressure. However, a change in pressure results in a change in the droplet size, which is not recommended to prevent drift and runoff. The ideal situation entails changing spray flow according to the map while keeping the circuit pressure constant at the magnitude that produces the appropriate droplet size. This need is behind the interest of PWM actuators, as flow can be regulated by changing the width of a pulse, technically known as the duty cycle (DC), but due to the frequency of the actuator, pressure changes are limited within an acceptable range that keeps droplet size acceptable. Figure 5 illustrates the working principles of a PWM nozzle with solenoids actuating at 10 Hz, which corresponds to cycles of 0.1 s. A duty cycle of 100% is equivalent to a nozzle permanently open, and likewise, nozzles are closed when DC is 0%. Any DC between 0% and 100% will, theoretically, output a spray flow proportional to the pulse width; therefore, smart sprayers will convert map

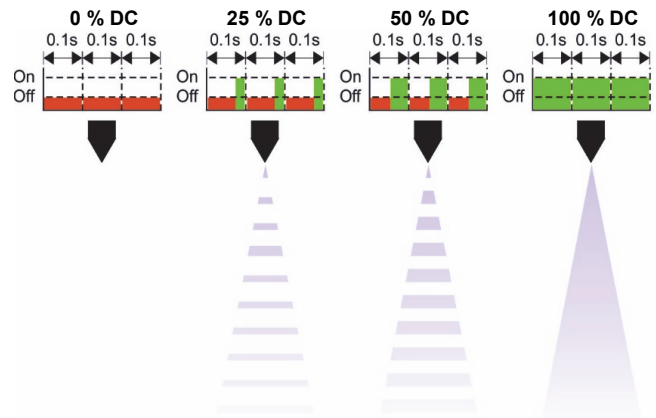


Figure 5. Principles of spray rate regulation with pulse width modulated solenoid valves.

flows into specific DC as indicated in the last step of the schematic of figure 4. However, the actual implementation of PWM nozzles tends to reduce their operational range, as found in the study cases presented below, which demonstrated that DC below 20% did not open the valves, DC above 80% fully opened the valves, the rate output by a 100% DC was significantly inferior to the flow advertised by the manufacturer for the same nozzle in conventional sprayers, and the straight association of percentage of DC to percentage of flow related to the maximum was not accurate (Saiz-Rubio et al., 2023). As a result, the practical implementation of the algorithm of figure 4 requires knowledge in detail of both the hydraulics and the electromechanical actuation for each intelligent sprayer.

## RESULTS

### VALIDATION CASE FOR CONTINUOUS TRELLISED CROPS: VINEYARDS

The first use case where the methodology was evaluated focused on the trellis-structured vineyards and the vineyard sprayer of figure 6. The air-assisted sprayer was customized to host 24 solenoid shutoff valves (TeeJet Technologies, Glendale Heights, IL, USA) distributed in four vertical



Figure 6. Validation of open-format prescription maps with a vineyard sprayer and trellised canopies.

sectors of six nozzles each with hollow disc cones (Albuz, Évreux, France), as the two external sectors were disconnected to only cover the two rows adjacent to the vehicle. The solenoid valves worked at 10 Hz and regulated the flow by varying the width of the pulse according to figure 5, being pressure limited to 10 bar to protect the solenoids. In addition, several sensors to monitor pressure and spray flow were integrated into the sprayer, as detailed in Saiz-Rubio et al. (2023).

A prescription map of 11,234 points based on vine vigor determined by an AUV was uploaded to the sprayer computer. The methodology used to calculate specific volume rates is based on the leaf wall area (LWA) concept proposed by the EPPO (European and Mediterranean Plant Protection Organization), the canopy density, the canopy width, and the type of sprayer (Gil et al., 2019). The spatial variation of the canopy structure required to apply this methodology was obtained from a canopy vigor map based on NDVI measurements acquired by a UAV equipped with a multispectral camera, yielding a resolution of 5 cm/pixel. Distinct vigor zones were correlated to canopy parameters through manual measurements at various points of the field for each labeled zone. Figure 7a plots the location of the reference points already transformed to LTP coordinates, whereas figure 7b shows the grid-based prescription map that resulted of

applying the mapping algorithm of equations 1-3 to the list of points depicted in figure 7a. Table 1 summarizes the key parameters involved in the construction of the (variable rate) prescription map according to the procedure described in this paper.

The sprayer shown in figure 6 was driven on 28 July 2022 along 30 vineyard rows spaced 2 m apart and at an average speed of 6.5 km/h. The rows had an orientation in headings of 25° and 205°, covering most of the prescription map outlined in figure 7b according to the trajectory map plotted in figure 8a. The spraying operation lasted 95 minutes, during which the rates prescribed in figure 7b were temporally

Table 1. Key parameters related to the construction of figure 7 prescription map.

Parameter	Value
Number of points (NP)	11,243
$E_{\min}$ (m)	-167.0
$E_{\max}$ (m)	147.2
$N_{\min}$ (m)	-181.1
$N_{\max}$ (m)	111.9
Map area (ha)	9.2
Map density (points/ha)	1,221
$c$ (m)	3
H (cells)	105
V (cells)	98
File size (kilobyte)	349

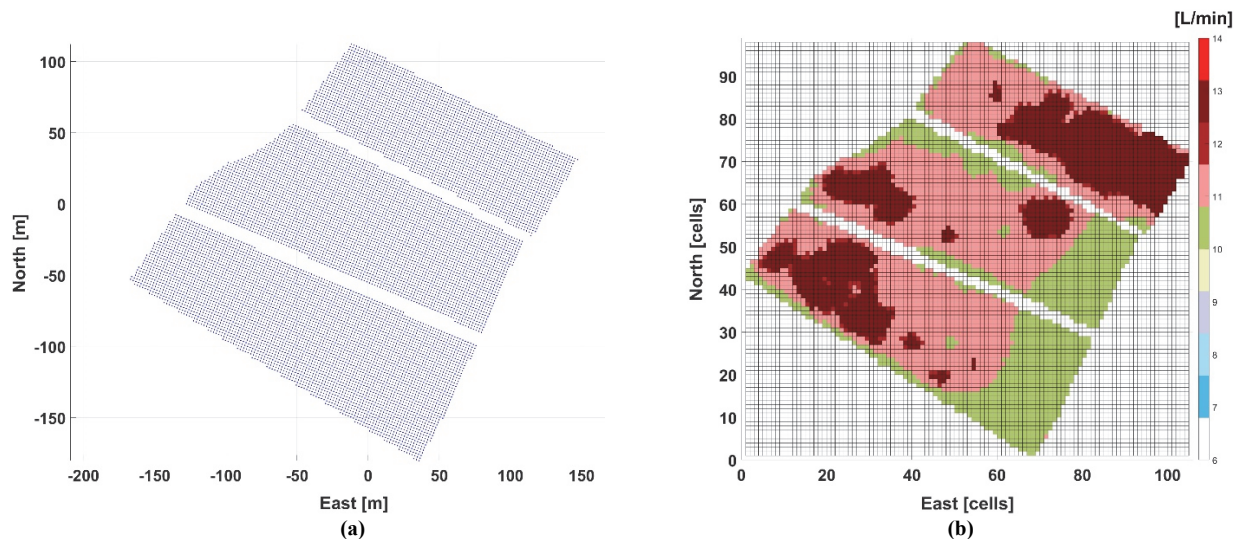


Figure 7. Construction of prescription maps: (a) generating points; (b) global-referenced prescription grid.

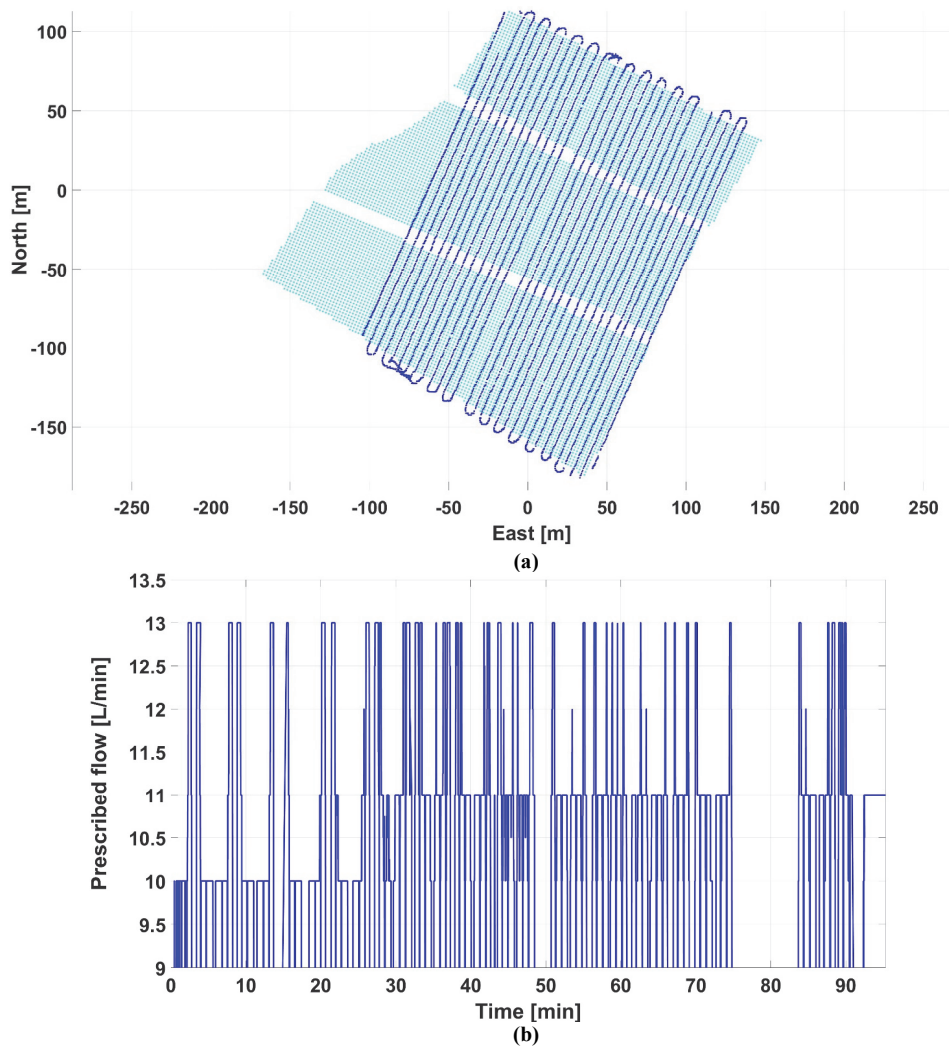


Figure 8. Trajectory followed by the sprayer (a) and flows (b) prescribed with time from the uploaded map.

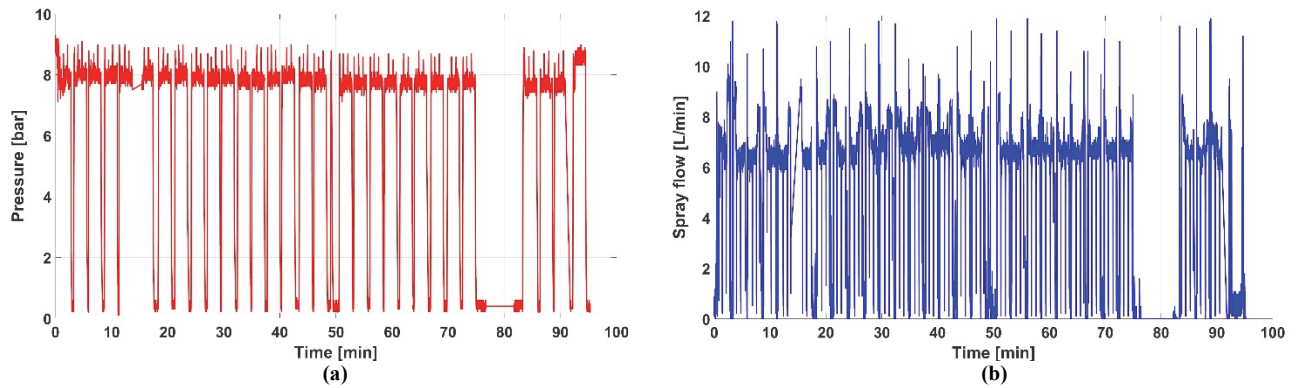


Figure 9. Sprayer key parameters: (a) Pressure (bar); (b) Flow measured with the sprayer flowmeter (L/min).

distributed according to figure 8b, with flows prescribed between 10 L/min and 13 L/min.

Figure 9 depicts the key parameters involved in the spraying operation: the actual flow measured by the flowmeter installed in the sprayer (fig. 9a), which sets how close the actual rates were to the prescribed rates; and the pressure profile (fig. 9b), which assures that droplet size falls within acceptable ranges. Even though flow variations were

physically executed by the sprayer and low-rate areas received less spray than high-rate areas, measured flow magnitudes were consistently below the prescribed rates. Figure 10a represents the spatial distribution of prescribed flow rates (from fig. 7b) for the specific area covered by the vehicle (81 x 99 cells), and figure 10b represents the actual flow rates executed in the field; when compared, zoning was very similar in both maps, being the deviation just in the amount



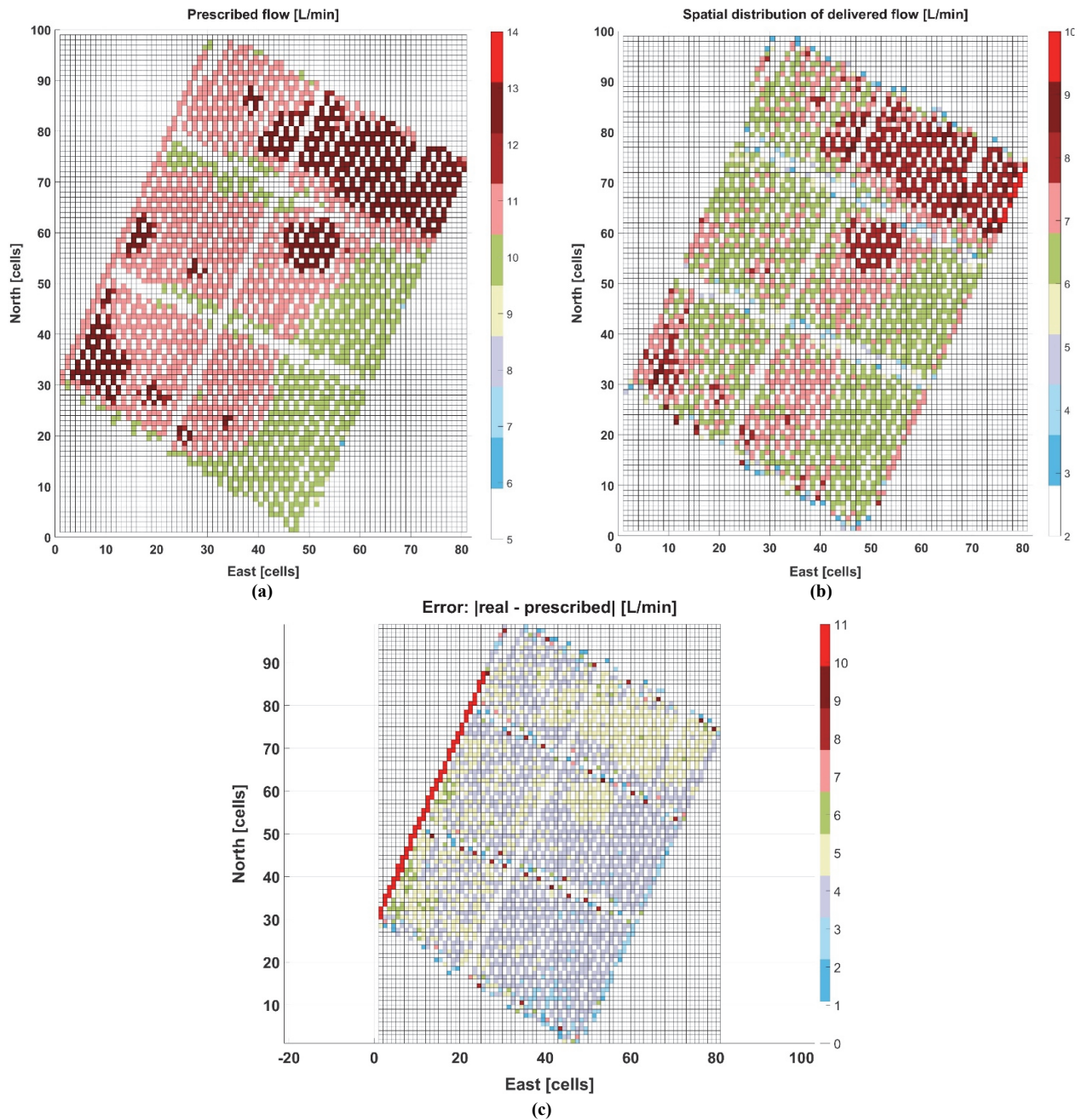


**Figure 10. Spatial distribution of spray treatment: (a) commanded flows; (b) flowmeter measurements; (c) deviations between prescribed and applied rates.**

of spray delivered. In particular, the distribution of such deviations were almost constant with an offset bias of 4 – 5 L/min, as represented in the histogram of figure 11. Numerically, the average error in the application was 4.14 L/min, with a standard deviation of 1.65 L/min. The error plot of figure 10 indicates that the error in flow was basically the same in the entire field, and therefore the correspondence between valve actuation and flow delivery should have been better matched to eliminate the offset. Two causes may explain these deviations in flow, none of which originated by the map layout. First, the majority of flowmeters are designed to work under laminar flows, losing accuracy when challenged by the highly pulsating phenomenon of PWM valves actuating at 10 Hz, mainly for virulent duty

cycles in the range 30% to 60%. The oscillating pattern of figure 9b shows that the measurements yielded by the onboard flowmeter were constantly varying from minimum to maximum values without reaching a steady state, which would be expected when the sprayer moved within zones of identical prescription. Second, the choice of nozzles was not accurate enough from the hydraulics standpoint. Nozzles should have delivered flows over 15 L/min for an average pressure of 8 bar according to manufacturer tables, such that top prescribed flows of 13 L/min (fig. 8b) could be reached when solenoids were actuated by duty cycles under 85%. Nevertheless, the right selection of nozzles is usually easy to correct given the large amount of commercial products readily available, but accuracy from the flowmeter should be

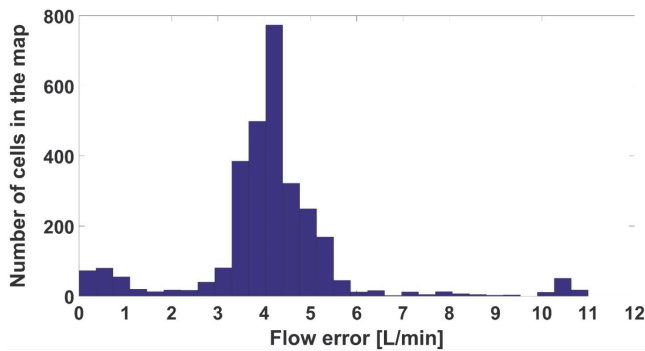


Figure 11. Histogram of absolute errors for the maps of figure 10.

granted for the practical range of operative duty cycles between 20% and 80%. Figure 10 shows that user prescriptions can be effectively taken to the field with the proposed mapping procedure as long as hydraulic adaptations in the sprayer reduce the deviations between the flowrates commanded through the prescription maps and the delivered ones. In particular, specific guidelines for nozzle selection and hydraulic adjustments that could make this methodology more actionable include the introduction of shock absorbers to attenuate the effect of pulses on measuring (flow and pressure) sensors, the measurement of maximum flow for the selected nozzles at preset pressure, as maximum flows differ from advertised rates due to flow restrictions inherent to solenoid valves, and the coincidence of the flowrate desired range with the operative range of the valves, typically between DC 20% and DC 80%. The error map of figure 10c shows significant errors in the left boundary, as the system took some seconds to start spraying and the delivered flow was practically null.

#### VALIDATION CASE FOR TRADITIONAL ORCHARDS: OLIVE GROVES

The second use case for validating the proposed methodology focused on traditional olive groves and the popular air blast sprayer in figure 12. As in the vineyard sprayer, hollow disc-cone nozzle bodies (D10 disc and DC45 core, TeeJet Technologies, Glendale Heights, IL, USA) were coupled with solenoid shutoff valves (TeeJet Technologies, Glendale Heights, IL, USA) for PWM control on each nozzle body,



Figure 12. Validation of prescription maps with an air blast sprayer in traditional olive groves.

closing and opening each valve when the solenoid was energized at a 10 Hz frequency. The regular battery of the pulling tractor provided 12 V and 30 A for powering the 16 solenoids on the sprayer. An additional battery supplied 12 V to run the onboard computer, a data acquisition card (National Instruments, Austin, TX, USA), a 14-inch touchscreen monitor hosting the graphic user interface (GUI) that operates the VR system, and a GPS receiver (SXblue, Anjou, QC, Canada). A pressure sensor (Wika, Klingenberg, Germany) and a flowmeter (Ifm Electronic, Essen, Germany) were mounted in the sprayer, as detailed in Orti et al. (2022).

A prescription map of 2,302 points based on the structure and vigor of olive trees was uploaded to the sprayer computer. As in the case of the vineyard, volume rates depended upon tree morphological characteristics (canopy volume and production type), but unlike the vineyard case, canopy volume was determined by a lidar sensor and ground-evaluated at significant field locations. Figure 13a plots the location of the reference points of the map already transformed to LTP coordinates, and figure 13b shows the grid-based prescription map that resulted from applying the mapping algorithm of equations 1-3 to the points depicted in figure 13a. Table 2 summarizes the key parameters involved in the construction of the variable rate map according to the proposed procedure.

The orchard sprayer depicted in figure 12 was operated in the northwest corner of the field along 15 rows at an average speed of 5 km/h, taking 26 minutes to apply the variable rate treatment. Figure 14a traces the trajectory of the sprayer, revealing a row spacing of 8 m. The average pressure along the treatment was 9 bar. Figure 14b plots the temporal application of flow rates according to the prescription map of figure 13b. Notice that the flows prescribed reached 45 L/min, are several times higher than the flows prescribed for the vineyard in figure 7b, revealing an important difference between both systems: traditional olive trees with much larger canopies demand larger flows, complicating the actuation of solenoid valves and the accurate measurement of flows with conventional flowmeters. The challenges of large flows for PWM-actuated nozzles are twofold: flowmeters are significantly more expensive and more sensitive to high-frequency pulses, compromising their reliability and lifespan; and on the other hand, large flows result in more virulent hammer shocks when full sectors are suddenly closed, typically at the headlands or with missing trees. In addition, as maximum advertised flows are not always available due to solenoid valve internal restrictions, high rates may require increasing the number of nozzles per sector to reach prescribed rates, which in turn leads to more expensive equipment.

A useful feature of the methodology proposed is the capability of users to adapt map resolution to their needs by simply changing the cell size  $c$ . This option was not necessary in the previous study case on vineyards, but a decrease in cell size was convenient for the case of many traditional orchards as higher resolution highlighted the location of tree rows. When comparing map density (tables 1 and 2), the vineyard map has 1,221 points/ha, whereas the olive orchard has 80 points/ha. Such a large difference has an impact on the size of the square cell automatically computed by the algorithm: 3 m for the vineyard (9 m<sup>2</sup>) versus 12 m for the



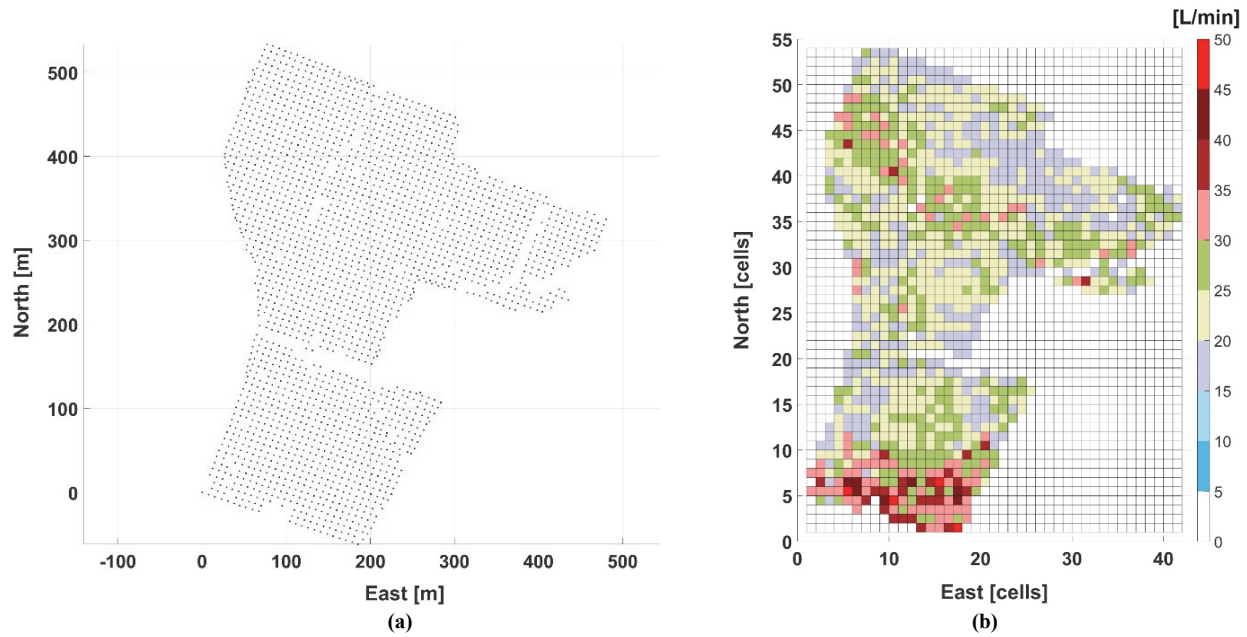


Figure 13. Olive grove prescription map: (a) generating points; (b) global-referenced prescription grid.

Table 2. Key parameters related to the construction of figure 13 prescription map for an olive grove.

Parameter	Value
Number of points (NP)	2,302
$E_{min}$ (m)	-2.2
$E_{max}$ (m)	478.1
$N_{min}$ (m)	-28.2
$N_{max}$ (m)	567.1
Map area (ha)	28.59
Map density (points/ha)	80
$c$ (m)	12
$H$ (cells)	41
$V$ (cells)	50
File size (kilobyte)	87

orchard ( $144 \text{ m}^2$ ). In order to assess the performance of the sprayer when applying a prescribed treatment coded with the proposed map format, it is necessary to keep the same resolution for the prescribed rates map and for the actually applied rates map, such that a cell-to-cell comparison may be carried out to estimate spray errors (fig. 16a). As sprayer sensors provide continuous measurements at the onboard computer cycle ( $\approx 2 \text{ Hz}$ ), there were significantly more points measured in the field during the treatment than the prescription-associated points of figure 13a. That is the reason why the prescription map of figure 13b has no blank cells in contrast to the map of figure 15a, even though both maps hold the same information. As a matter of fact, the map of figure 15a has been depicted from the same data source that led to the map of figure 13b, namely the list of reference points introduced by the user with the format of figure 1. Notice how the higher resolution map of figure 15 outlines the 16 rows followed by the vehicle in figure 14a. The cell-to-cell comparison of both maps in figure 15 allows the estimation of the relative errors in figure 16a, which yields a closer adjustment in flow between prescribed and delivered rates than the vineyard case. Blank cells in the map of figure 16a represent either cells without data (space between rows) or cells with a relative error below 10%. In terms of absolute

errors, figure 17 provides the histogram that explains the distribution of errors (L/min) for the 1,200 cells of the grid labeled with a measured flow, out of the 5,346 cells that make the full map. The solenoid actuation map of figure 16b reveals that the solenoids were actuated by duty cycles between 30% and 80%, which covers the full operational range of the implemented solenoids and thus makes an advantageous use of PWM technology as the most promising driver to date of variable rate applications.

## DISCUSSION

This research presents and explains a novel methodology to construct prescription maps for the practical application of precision agriculture principles. The originality of this methodology roots in a straightforward procedure to code variable rates in a plain format that is independent of any manufacturer and therefore can be easily (and freely) applied by both users and industry. This methodology has been validated for spraying in orchard crops, which pose serious challenges to the application of variable rates due to the demand of higher pressure and flow than in field crops. The method presented here explains how to take variable rates to the field in a systematic procedure but does not cover the calculation of rates, which depends on the specific features of each crop and its supporting system. Therefore, before coding prescription maps with this procedure, growers need to understand how variable rating works and the importance of drift prevention, but once coding has been eased with the algorithms proposed in figure 3, the focus will mostly be on precision and efficiency.

An important decision for a user writing a prescription map in the format of figure 1 is the selection of the number of points NP, as it influences the cell size and thus the resolution of the map. The algorithm of figure 3 calculates the optimal cell size  $c$  to provide full coverage of the plot,

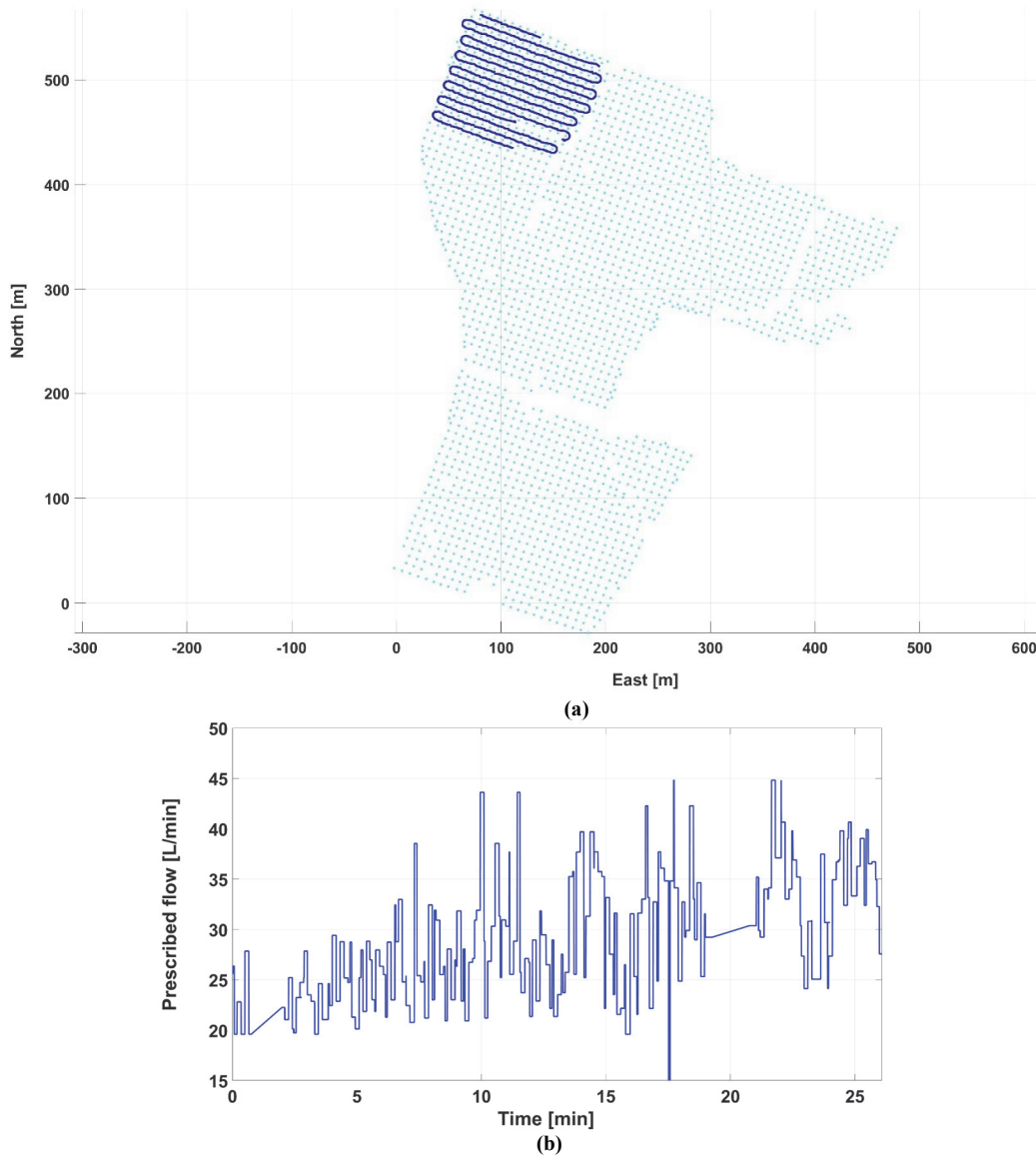


Figure 14. Trajectory followed by the sprayer (a) and flows prescribed with time from uploaded map (b).

considering that the points sampled by the user are evenly distributed in the field plot. For the case of continuous trellised rows, high map resolution will result in more variations of the duty cycle with time, but as PWM valves will be continuously actuating at 10 Hz, the system will execute the prescribed rates without problems regardless of the resolution. In the case of isolated trees within rows, however, the resolution may have a significant effect. If the cell size is significantly larger than the spacing between adjacent trees, the system will behave as the continuous trellis case because all the cells will normally have a rate assigned to them. But if the grid resolution is very high (tree-specific and beyond), the blank cells between adjacent trees will shut off solenoid valves completely, which will require the hydraulic system of the sprayer to instantaneously release the sudden rise of pressure to avoid causing damage to the solenoid valves. The olive trees use-case presented in this article registered sudden pressure increases of 4 bar that fired a discharge safety valve, effectively protecting the 16 solenoid valves of the

sprayer, whose working pressure is limited to 10 bar. However, a more sophisticated multiple-stage return line might have kept pressure within a safe range regardless of DC assignment, preventing the less stable firing of the discharge valve.

The simple layout proposed for coding a prescription map (fig. 1) has the advantage of working for any field regardless of its size, thus helping to introduce precision farming in smallholdings and counterweight the reluctance of conventional farmers to adopt VRT, as found by Masi et al. (2023). The majority of orchard crop farms in Europe are small and medium size. In fact, small plots require fewer points (NP), which makes the writing of the maps even easier. The introduction of digitization in agriculture requires more intense training for the 21<sup>st</sup> century farmer (Saiz-Rubio and Rovira-Más, 2020), but once the routine of map writing has been learned, the elaboration of prescription maps with this methodology becomes automatic. The spray rates prescribed in the maps of figures 7b and 13b have been expressed in L/min



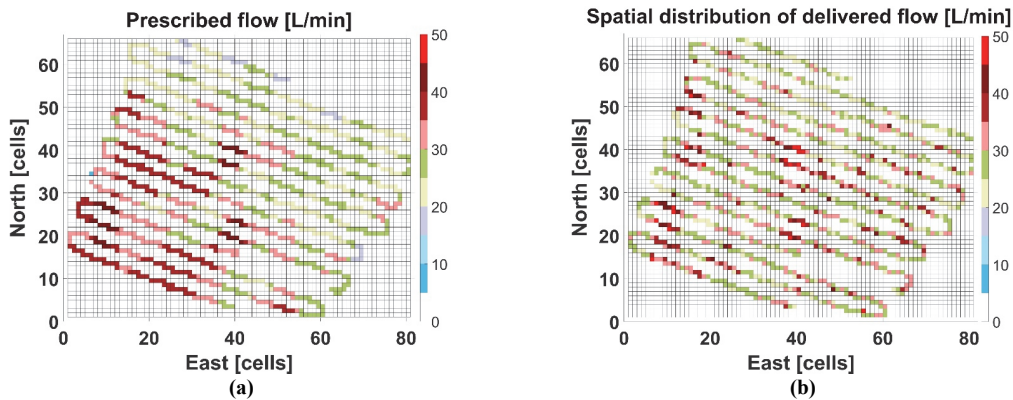


Figure 15. Spatial distribution of spray treatment: (a) commanded flows; (b) flowmeter measurements.

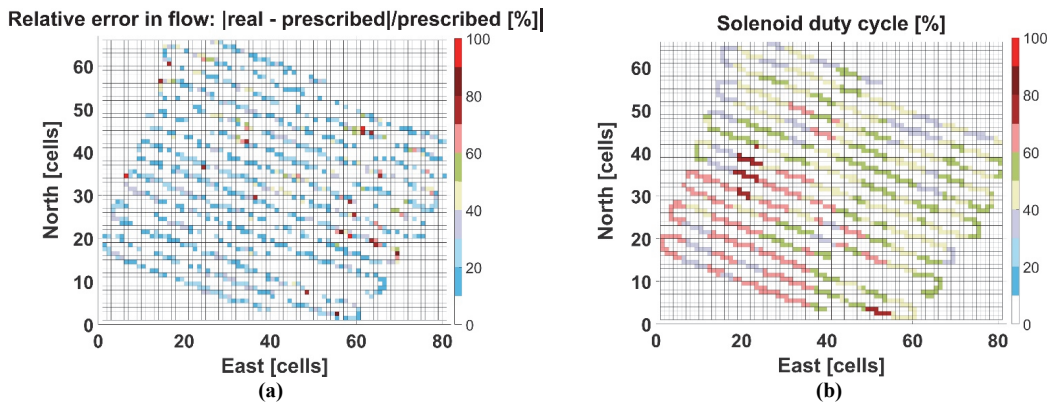


Figure 16. Spatial distribution of (a) relative spraying error (%) and (b) solenoid actuation (%).

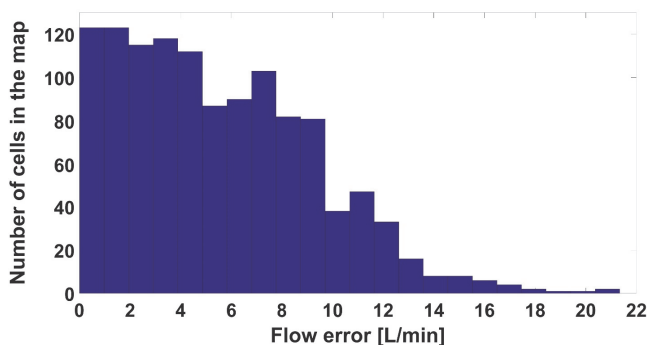


Figure 17. Histogram of absolute errors for the maps of figures 15 and 16.

for convenience and consistency; however, many farmers are used to managing spray rates in L/ha. If a map is preferred in L/ha, it can be instantaneously transformed to L/min (necessary to determine the DC of the valves) as long as the row spacing and the vehicle speed are known. Row spacing can be input to the system by the sprayer operator and will usually remain constant over the treatment. However, the vehicle speed will likely vary along the rows and should be measured in real time, for example, with the onboard GPS, to fine-adjust the rate in L/min on-the-fly.

The precise delivery of time-varying spray rates is not straightforward due to complex PWM dynamics and valve-wearing hydraulic effects, such as hammer shocks when solenoid valves are quickly closed, a typical behavior found when sprayers stop spraying along gaps between trees for

high-resolution maps of traditional orchards. Unfortunately, this operational complexity can be common in conventional orchard crops not supported by trellised structures. A complete variable-rate spraying operation must consider both the digital handling of data and the physical inertias of actuators and moving liquids. In the use cases presented in this article, the flow rate was regulated in real time, but a constant pressure over the entire process, and thus a constant droplet size, could be guaranteed only within a certain range. The pulsating effect of numerous PWM solenoid valves actuating simultaneously (24 in the vineyard sprayer and 16 in the blast sprayer) had an impact on key system sensors, most of which are designed for laminar flows. Pressure must be accurately measured to grant the appropriate droplet size for all the treatment, and the timely supply of the prescribed flow for any field location is the guarantee to avoid drift and runoff, as demanded by environmental agencies. The sprayers were modified to include redundant pressure gauges capable of tracking instantaneous pressure, but in spite of protecting sensors with shock absorbers, several pressure sensors broke, and the flowmeter measurements oscillated significantly as a consequence of 10 Hz pulses. Rather than modifying a conventional sprayer to feature variable rating, a new conceptual design with customized hydraulic circuitry that accommodates high frequency actuators would likely increase performance and cost-efficiency. Nevertheless, the application of variable rates according to user-defined prescriptions encoded with the proposed methodology was demonstrated for crops with diverse supporting systems.

Future steps to promote commercialization will result in a more sophisticated flow-return system to keep pressure within a reduced interval regardless of any actuation at nozzle level, such that system pressure can be pre-calibrated to the optimum magnitude according to the droplet size, and thus growers can be released from tampering with pressure regulators. Once pressure and flow are effectively controlled by a smart system, users can focus on what really matters for them: deciding the right amount of spray that each tree needs for sustainable management of the crop.

## CONCLUSIONS

The lessons learned from the 3-year project supporting the research reported in this paper can be summarized in the following points:

- The reduction rates of crop protection products currently imposed by environmental agencies require the introduction of smart solutions such as variable rate technologies (VRT). However, the lack of standardization and straightforward procedures is a barrier for the practical implementation of VRT. At present, each manufacturer uses its own prescription map format and firmware.
- Spatial resolution is crucial when coding spray prescriptions for VRT. The developed methodology eases the way of handling resolution through the selection of the number of points (NP) decided by the user and the automatic determination of the cell size (c) calculated by the algorithm. As a result, the proposed format offers a simple layout for coding a prescription map in a text format without the need of specific software; in fact, the text may be written in any word processor.
- The highly pulsating effect of PWM valves had negative consequences on sensor performance and durability, which complicated the monitoring and evaluation of the sprayer actuation. The accuracy of VRT spray applications requires flowmeters that are precise under the demanding conditions of PWM nozzles. Without reliable flowmeters, it is not feasible to decouple the effect of poor valve actuation from poor sensor measurements. Part of the error contained in the histogram of figure 17 should, for instance, be attributed to the lack of robustness of the onboard flowmeter. In general, the handling of PWM nozzles for orchards not arranged in regular trellises brings additional complexities to the solutions already developed for boom sprayers due to the lack of continuity in foliage, the need for larger pressures, and the extended range of operational flows.
- The variable application of pre-set rates according to user-defined prescriptions encoded with the proposed methodology was successfully demonstrated with regular equipment in commercial orchards: *spray rates varied in real time based on a pre-defined map with minor changes in circuit pressure*. As this methodology facilitates the implementation of VRT, a technique to apply precision farming in

practice, the advantages of precision farming will be promoted as well, in particular the economic and environmental benefits of a better adjustment of volume rates. Optimized rates will prevent drift to the atmosphere, runoff to the soil, and heavy expenses in pesticides by the farmer, as VRT has been proven to reduce pesticide or fungicide use up to 30%-40%. For the vineyard case studied in this article, the reduction of crop protection products was estimated at 35% for the 2023 season, although some reduction was partially due to smaller canopies resulting from a dry season. Nevertheless, although the initial investment required for VRT equipment is typically higher as a consequence of electronic equipment such as sensors, computers, and solenoid valves, significant product savings will occur on a yearly basis, and thus the investment in VRT may be recovered in several years. The exact return of investment, however, is difficult to assess in general, as these systems are still new and each farming situation is different.

## ACKNOWLEDGMENTS

The authors would like to thank F. García and R. Salcedo (UPC) for map construction and field validation tests in vineyards, and A. Rodríguez-Lizana and J. M. Mariscal for map construction and field validation tests in olive groves (UCO). This research has been funded by national projects PIVOS (PID2019-104289RB) and ADOPTA (PDC2022-133395-C42).

## REFERENCES

- Brown, R. B., & Steckler, J. P. (1995). Prescription maps for spatially variable herbicide application in no-till corn. *Trans. ASAE*, 38(6), 1659-1666. <https://doi.org/10.13031/2013.27992>
- Burks, T. F., Schmoldt, D. L., & Steiner, J. J. (2008). U.S. Specialty crops at a crossroad: Hi-tech or else? *Resource Magazine*, 15(6), 5-6. Retrieved from <https://elibrary.asabe.org/abstract.asp?aid=29280&t=11>
- Fabula, J., Sharda, A., Kang, Q., & Flippo, D. (2021). Nozzle flow rate, pressure drop, and response time of pulse width modulation (PWM) nozzle control systems. *Trans. ASABE*, 64(5), 1519-1532. <https://doi.org/10.13031/trans.14360>
- FAO. (2023). FAOSTAT - Crops and livestock products. Retrieved from <https://www.fao.org/faostat/en/#data/QCL>
- Gil, E., Campos, J., Ortega, P., Llop, J., Gras, A., Armengol, E.,... Gallart, M. (2019). DOSAVIÑA: Tool to calculate the optimal volume rate and pesticide amount in vineyard spray applications based on a modified leaf wall area method. *Comput. Electron. Agric.*, 160, 117-130. <https://doi.org/10.1016/j.compag.2019.03.018>
- Grewal, M. S., Weill, L. R., & Andrews, A. P. (2001). *Global positioning systems, inertial navigation, and integration*. New York: John Wiley and Sons. <https://doi.org/10.1002/0471200719>
- Han, S., Hendrickson, L. L., Ni, B., & Zhang, Q. (2001). Modification and testing of a commercial sprayer with PWM solenoids for precision spraying. *Appl. Eng. Agric.*, 17(5), 591. <https://doi.org/10.13031/2013.6906>
- Li, S., Chen, Y., Wan, C., Zheng, Y., Yang, L., & Liu, H. (2019). Design of software of prescription map for precise fertilization. Paper no. 1901048. *Proc. 2019 ASABE Annu. Int. Meeting*. St. Joseph, MI: ASABE. <https://doi.org/10.13031/aim.201901048>

- Masi, M., Di Pasquale, J., Vecchio, Y., & Capitanio, F. (2023). Precision farming: Barriers of variable rate technology adoption in Italy. *Land*, *12*(5), 1084. <https://doi.org/10.3390/land12051084>
- Norwood, S. H., Winstead, A., & Fulton, J. (2009). Introduction to prescription maps for variable-rate application, ANR-1362. Alabama Cooperative Extension System.
- Ortí, E., Cuenca, A., Pérez, M., Torregrosa, A., Ortiz, C., & Rovira-Más, F. (2022). Preliminary evaluation of a blast sprayer controlled by pulse-width-modulated nozzles. *Sensors*, *22*(13), 4924. <https://doi.org/10.3390/s22134924>
- Ortiz, C., Torregrosa, A., Saiz-Rubio, V., & Rovira-Más, F. (2023). Vibration analysis of pulse-width-modulated nozzles in vineyard blast sprayers. *Horticulturae*, *9*(6), 703. <https://doi.org/10.3390/horticulturae9060703>
- Rathnayake, A. P., Sahni, R. K., Khot, L. R., Hoheisel, G. A., & Zhu, H. (2022). Intelligent sprayer spray rates optimization to efficiently apply chemicals in modern apple orchards. *J. ASABE*, *65*(6), 1411-1420. <https://doi.org/10.13031/ja.14654>
- Rovira-Más, F., Zhang, Q., & Hansen, A. C. (2010). *Mechatronics and intelligent Systems for off-road vehicles*. London, UK: Springer-Verlag. <https://doi.org/10.1007/978-1-84996-468-5>
- Saiz-Rubio, V., & Rovira-Más, F. (2020). From smart farming towards agriculture 5.0: A review on crop data management. *Agronomy*, *10*(2), 207. <https://doi.org/10.3390/agronomy10020207>
- Saiz-Rubio, V., Ortiz, C., Torregrosa, A., Ortí, E., Pérez, M., Cuenca, A., & Rovira-Más, F. (2023). Modelling vineyard spraying by precisely assessing the duty cycles of a blast sprayer controlled by pulse-width-modulated nozzles. *Agriculture*, *13*(2), 499. <https://doi.org/10.3390/agriculture13020499>
- Salcedo, R., Zhu, H., Zhang, Z., Wei, Z., Chen, L., Ozkan, E., & Falchieri, D. (2020). Foliar deposition and coverage on young apple trees with PWM-controlled spray systems. *Comput. Electron. Agric.*, *178*, 105794. <https://doi.org/10.1016/j.compag.2020.105794>
- Song, P., Lan, Y., Li, W., & Fang, X. (2012). Prescription maps for precision aerial application. Paper no. 121338453. *Proc. 2012 ASABE Annu. Int. Meeting*. St. Joseph, MI: ASABE. <https://doi.org/10.13031/2013.42193>
- Yang, C., Odvody, G. N., Thomasson, J. A., Isakeit, T., Minzenmayer, R. R., Drake, D. R., & Nichols, R. L. (2018). Site-specific management of cotton root rot using airborne and high-resolution satellite imagery and variable-rate technology. *Trans. ASABE*, *61*(3), 849-858. <https://doi.org/10.13031/trans.12563>